Concerted Conformational Effects of Ca^{2+} and ATP Are Required for Activation of Sequential Reactions in the Ca^{2+} ATPase (SERCA) Catalytic Cycle[†,‡]

Giuseppe Inesi,* David Lewis, Hailun Ma, and Anand Prasad

California Pacific Medical Center Research Institute, 475 Brannan Street, San Francisco, California 94107

Chikashi Toyoshima

Institute of Molecular and Cellular Biosciences, University of Tokyo Bunkyo-ku, Tokyo 113-0032, Japan

Received June 23, 2006; Revised Manuscript Received September 11, 2006

ABSTRACT: We relate solution behavior to the crystal structure of the Ca^{2+} ATPase (SERCA). We find that nucleotide binding occurs with high affinity through interaction of the adenosine moiety with the N domain, even in the absence of Ca^{2+} and Mg^{2+}, or to the closed conformation stabilized by thapsigargin (TG). Why then is Ca^{2+} crucial for ATP utilization? The influence of adenosine 5′-(β,γ-methylene) triphosphate (AMPPCP), Ca^{2+}, and Mg^{2+} on proteolytic digestion patterns, interpreted in the light of known crystal structures, indicates that a Ca^{2+}-dependent conformation of the ATPase headpiece is required for a further transition induced by nucleotide binding. This includes opening of the headpiece, which in turn allows inclination of the "A" domain and bending of the "P" domain. Thereby, the phosphate chain of bound ATP acquires an extended configuration allowing the γ-phosphate to reach Asp351 to form a complex including Mg^{2+}. We demonstrate by Asp351 mutation that this "productive" conformation of the substrate−enzyme complex is unstable because of electrostatic repulsion at the phosphorylation site. However, this conformation is subsequently stabilized by covalent engagement of the γ-phosphate yielding the phosphoenzyme intermediate. We also demonstrate that the ADP product remains bound with high affinity to the transition state complex but dissociates with lower affinity as the phosphoenzyme undergoes a further conformational change (i.e., E1−P to E2−P transition). Finally, we measured low-affinity ATP binding to stable phosphoenzyme analogues, demonstrating that the E1−P to E2−P transition and the enzyme turnover are accelerated by ATP binding to the phosphoenzyme in exchange for ADP.

The Ca^{2+} ATPase of Sarco/Endoplasmic Reticulum (SERCA)[1] is a membrane-bound enzyme that uses ATP as an energy source for Ca^{2+} transport. The 100 kDa ATPase protein includes 10 helical segments partitioned within the membrane bilayer and a headpiece protruding from the cytosolic membrane surface (*1*, *2*). Binding of 2 Ca^{2+} is required for enzyme (E) activation, whereby the ATP terminal phosphate is utilized to form a phosphorylated enzyme intermediate (E-P). The bound Ca^{2+} then undergoes occlusion and vectorial translocation. The catalytic cycle is completed by hydrolytic cleavage of E-P (*3*−*5*).

The Ca^{2+}-binding domain and the ATP/catalytic site are separated by a rather large distance within the ATPase molecule, as the former resides within the membrane-bound region of the enzyme and the latter within the headpiece outside the membrane. Therefore, coupling of ATP utilization and Ca^{2+} transport requires a "long range intramolecular linkage" (*6*) operated by protein conformational changes. Evidence of protein conformational changes following Ca^{2+} and ATP binding was first obtained by spectroscopic studies (*7*). Atomic models of the ATPase structure were then developed (*8*−*14*) demonstrating diverse conformational states derived from crystals obtained in the absence of Ca^{2+} (stabilized by thapsigargin: E2−TG), in the presence of Ca^{2+} (E1−2Ca^{2+}), and in the presence of high concentrations of substrate and/or products yielding stable analogues of catalytic cycle intermediates (Figure 1).

Ca^{2+} binding to the ATPase is an absolute requirement for ATP utilization, and ATP is utilized at micromolar concentrations by the Ca^{2+}-activated enzyme. However, plots of steady-state rates of ATP hydrolysis yield a further increase of velocity at higher ATP concentrations (*15*−*18*), raising the question of a second (i.e., activating) ATP site. A number of amino acid residues involved in ATP binding and formation of the phosphoenzyme intermediate were identified by protein chemistry (*19*−*21*) and mutational analysis (*22*−*26*). Involvement of these residues is consistent with recent crystallographic studies including the ATP analogue adenosine 5′-(β,γ-methylene) triphosphate (AMPPCP) or ADP and fluoroaluminate (*10*, *12*, *14*). There are

[†] Supported in part by the NHBLI, National Institutes of Health Grant RO1 HL69830.

[‡] Initial experiments were conducted in the Biochemistry Department of the University of Maryland School of Medicine.

* Corresponding author. California Pacific Medical Center Research Institute, 475 Brannan Street, San Francisco, CA 94107. Tel, 415-6001745; fax, 415-6001725; e-mail, ginesi@cpmcri.com.

[1] Abbreviations: SERCA, sarco/(endo)plasmic reticulum Ca^{2+} ATPase; TG, thapsigargin; CPA, cyclopiazonic acid; TNP-ATP, 2′(3′)-*O*-(2,4,6-trinitrophenyl) adenosine 5′, triphosphate; WT, wild-type; EGTA, ethylene glycol bis-(β-amino ethyl ether)-*N*,*N*,*N*′,*N*′-tetraacetic acid; MOPS, 3-(*N*-morpholino) propanesulfonic acid; AMPPCP, adenosine 5′-(β,γ-methylene) triphosphate.

10.1021/bi061255d CCC: $33.50
Published on Web 10/26/2006

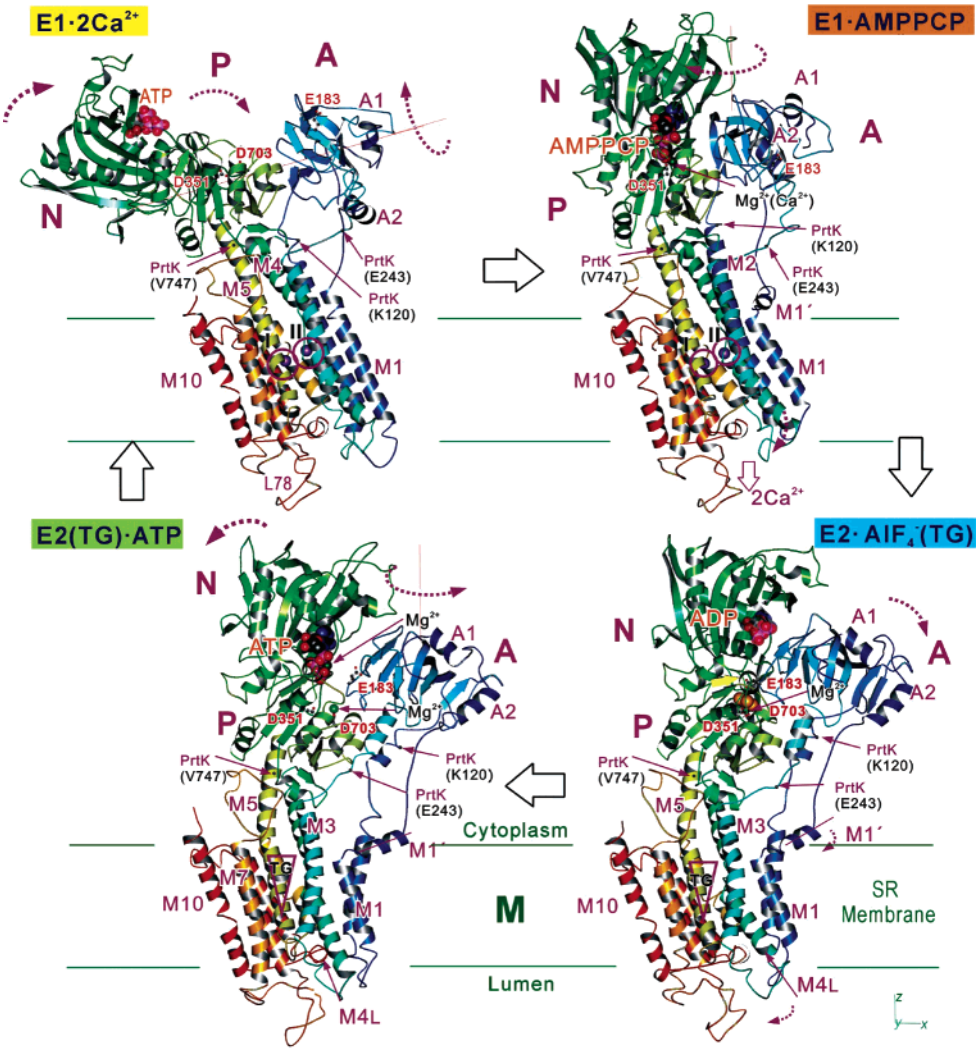

FIGURE 1: Conformational states of the Ca^{2+}-ATPase in the presence and absence of Ca^{2+}, substrate and product analogues, based on the coordinates deposited in PDB ID: 1SU4 (E1·$2Ca^{2+}$; (*8*)), 1VFP (E1·AMPPCP (*10*)), 1XP5 (E2·AlF_4^-(TG) (*13*)), and 2DQS and 2D88 (E2(TG)·ATP, (*14*)). ATP in E1·$2Ca^{2+}$ and ADP in E2·AlF_4^-(TG) are docked by fitting the N domain of E1·AMPPCP and E2·MgF_4^{2-}(TG) (PDB ID: 1WPG (*11*)). Color changes gradually from the N-terminus (blue) to the C-terminus (red). The two Ca^{2+} (I and II) bound to the high-affinity transmembrane sites are circled when present. Three key residues (E183 in the A domain, D351 and D703 in the P domain) are shown in ball-and-stick. Note the positional changes of headpiece domains in the various conformations, as well as the proteinase K sites (*30*) in the loops connecting the A domain to the M2 and M3 helices. Note the nucleotide binding to the N domain, and the variable relationship of the nucleotide phosphate chain (and Mg^{2+}) with the P and A domains.

however, outstanding issues regarding the requirements for ATP binding and, in turn, the effect of ATP binding on enzyme conformation. One issue is related to whether the open headpiece configuration of the enzyme in the presence of $2Ca^{2+}$ (E1−$2Ca^{2+}$), as opposed to the closed configuration in the absence of Ca^{2+} (E2−TG), has an influence on the access and binding affinity of ATP, and whether the presence of thapsigargin (TG) used for the stabilization of E2 makes any difference. Another issue is related to the orientation of the ATP phosphate chain and the conformation of the enzyme with bound nucleotide in solution. In fact, the enzyme with bound nucleotide (AMPPCP−E1−$2Ca^{2+}$) and the phosphoenzyme analogue with bound ADP (ADP−E1−AlF_x−$2Ca^{2+}$) yield quite similar crystal structures, including evidence for an occluded state of bound Ca^{2+} (*10*, *12*). In contrast, the effects of these ligands in solution are quite different (*27*, *28*), since Ca^{2+} occlusion can be easily demonstrated in the presence of AlF_x and ADP, but it is very difficult to demonstrate in the presence of AMPPCP. Finally, a related issue is the lack of any data on ADP binding by the ATPase in solution.

With the experiments reported here, we endeavored to obtain systematic measurements of ATP and ADP binding to the ATPase in sequential states of the catalytic cycle and to check related enzyme conformations by analysis of proteinase K digestion patterns *in solution* (*29*−*31*). This analysis of the protein is rendered possible by changes in exposure and flexibility of the proteolytic sites in concomitance with conformational changes of the ATPase protein (Figure 1), which can then be related to information available from crystallography. Considering the kinetic and structural information obtained so far, the binding constants and the conformational effects revealed by our experiments can be of significant help in understanding (1) whether and how ATP binds to the enzyme in the absence and in the presence of Ca^{2+}, and why it is utilized only in the presence of Ca^{2+}; (2) whether ATP binding may be expected to influence the kinetics of the cycle, in addition to direct utilization as

substrate; (3) whether ADP is a strong or weak ligand, and is a good leaving group following phosphoryl transfer from ATP to the enzyme; and (4) whether the ATPase headpiece conformation is affected by TG binding.

MATERIALS AND METHODS

Sarcoplamic retuculum (SR) vesicles were obtained from rabbit skeletal muscle (*32*). Recombinant Ca^{2+} ATPase was obtained from COS-1 cells infected with adenovirus vectors carrying chicken wild-type (WT) (*33*) or mutant cDNA (*34*).

ATP and ADP binding was measured by a filtration method (*35*−*37*). The reaction medium contained 40 mM MOPS, pH 7.0, 80 mM KCl, 2 mM $MgCl_2$, 1 mM EGTA (in the absence or in the presence of 1 mM $CaCl_2$), and various concentrations of [^{32}P]- or [^{14}C]-labeled nucleotide. For each experimental sample, 3 mL of ice-cold medium was added by fast mixing to 0.3 mL of medium containing 0.4 mg of SR protein and filtered after 10 s through a 0.65 μm Millipore filter. Controls were obtained by passing through the filters the same volume of reaction medium containing corresponding concentrations of nucleotide in the absence of SR protein. The filters were blotted and processed for scintillation counting. The radioactivity associated with control filters was subtracted from the radioactivity of samples containing SR protein. The radioactivity associated with the filters in the absence, as compared with the presence, of protein was approximately 10% at 1 μM ATP and up to 30% at 50 μM ATP. In some experiments, 2 mM KF and 0.1 mM $AlCl_3$ were added, and the reaction mixture was incubated for 30 min in order to obtain the fluoroaluminate complex, in the absence or in the presence of nucleotides. All binding curves were obtained by computer fitting, based on a single and independent site (noncooperative) binding equation.

Enzyme phosphorylation by ATP was measured at 2 °C with a reaction mixture containing 40 mM MOPS, pH 7, 80 mM KCl, 2 mM $MgCl_2$, 50 μM $CaCl_2$, 0.4 mg of SR protein/mL, and 2 μM A23187 ionophore. Individual samples (0.2 mL) were started by the addition of [γ^{32}P]ATP, and quenched with 1 M perchloric acid. Enzyme phosphorylation with P_i was obtained by equilibration (10 min at 25 °C) of SR vesicles (2.0 mg/mL) with 0.5 mM [γ^{32}P]P_i, in a medium containing 40 mM MES, pH 6.5, 3 mM $MgCl_2$, 1 mM EGTA, and 20% Me_2SO_4. The reaction was quenched with 1 M PCA. The quenched reaction mixture was filtered on 0.65 μm Millipore filters, and the protein collected on the filters was washed three times with 0.125 M perchloric acid, once with cold water, and finally dissolved with dimethylformamide and processed for scintillation counting. Control experiments were performed with nonradiolabeld ATP or phosphate in the perchloric acid quench to exclude the occurrence of noncovalent binding to the quenched protein.

Decay of radioactive phosphoenzyme obtained by incubation with 10 μM ATP for 10 s at 2 °C was initiated by a chase with 10 mM EGTA, or 10 mM EGTA and 1 mM nonradioactive ATP. Decay of radioactive phosphoenzyme obtained by incubation for 10 min at 25 °C with 0.5 mP_i was initiated by a chase with 50 mM nonradioactive P_i with or without 1 mM ATP. In both cases, the temperature of the chase was 2 °C. Samples were acid-quenched and processed for determination of radioactivity. The decay curves were analyzed by exponential computer fitting.

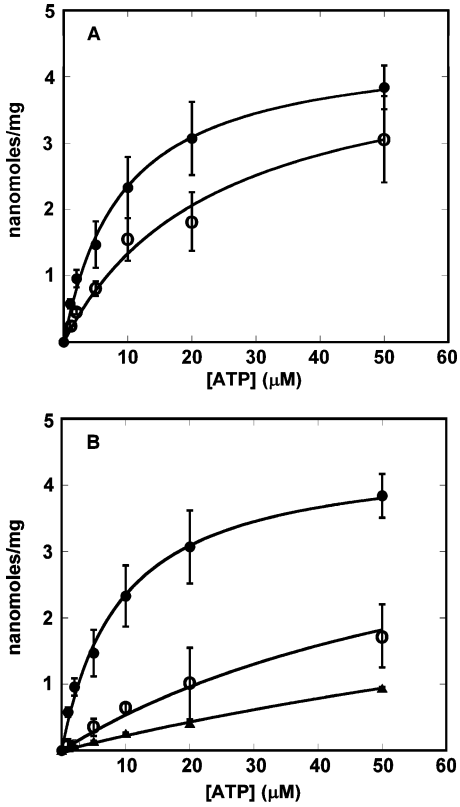

FIGURE 2: ATP binding to the ATPase in the absence of Ca^{2+}. (A) In the presence (●) and in the absence (○) of Mg^{2+}; (B) in the presence of Mg^{2+} (●), and following addition of 1 μM TG (○) or 100 μM CPA (▲). ATP was added rapidly to the medium at 2 °C, and the mixture was filtered after 10 s incubation as described in Materials and Methods.

Limited proteolytic digestion was performed in reaction mixtures containing 50 mM MOPS, pH 7.0, 50 mM NaCl, 0.4 mg of microsomal protein (COS-1 cell microsomes containing chicken recombinant SERCA)/mL, and 0.01−0.04 mg of proteinase K. $CaCl_2$, $MgCl_2$, EGTA, and AMPPCP were added as indicated in the figures. Following incubation at 25 °C for various time intervals, the reaction was quenched with trichloroacetic acid (2.5%), and the protein was solubilized with a medium containing sodium dodecyl sulfate (1%), MOPS (0.312 M), pH 6.8, sucrose (3.75%), β-mercaptoethanol (1.25 mM), and bromophenol blue (0.025%). The samples were then subjected to electrophoretic analysis on 12% gels. Western blots were obtained using the monoclonal antibody 5C3, followed by goat anti-mouse IgG horseradish peroxidase-conjugated secondary antibodies and visualization with an enhanced chemiluminescence-linked detection system (Amersham Biosciences).

RESULTS

ATP Binding to the ATPase in the Absence of Ca^{2+}. We measured ATP binding by mixing SR vesicles with various nucleotide concentrations and filtering after a 10 s incubation, since full substrate binding and utilization is expected within this time limit in the presence of Ca^{2+} (see below). In the binding experiments, however, we omitted Ca^{2+} to avoid ATP consumption and, thereby, obtained satisfactory binding isotherms (Figure 2A). Analysis of the experimental points demonstrates noncooperative binding yielding 5−9 μM K_d values at pH 7.0, and maximal levels of 4.5 nmol ATP/mg

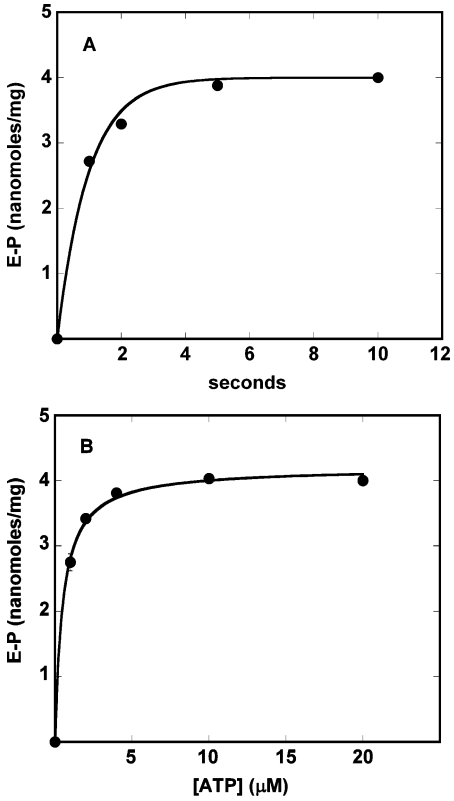

FIGURE 3: ATP utilization for formation of phosphorylated enzyme intermediate. (A) Time dependence; (B) ATP concentration dependence. The experiments were conducted at 2 °C by adding ATP (10 μM in panel A, as specified in panel B), and quenching at the time specified in panel A, or after 10 s incubation in panel B. Reaction mixture given in Materials and Methods.

protein. These levels correspond to the stoichiometry of ATPase in our microsomal preparation and indicate binding saturation. It is then clear that the enzyme can bind ATP even in the absence of Ca^{2+} (i.e., E2 state). The binding affinity observed in the absence of Ca^{2+} is consistent with the ATP concentration required for phosphoenzyme formation in the presence of Ca^{2+} (see below). Therefore, the absolute Ca^{2+} requirement for ATP utilization is not simply related to an effect of Ca^{2+} on the ATP binding affinity.

ATP binds to the enzyme even in the absence of Mg^{2+} (Figure 2A), although with lower affinity (K_d = 24 μM), indicating that neutralization of the phosphate charge is not strictly required for simple binding. It is of interest that (in the presence of Mg^{2+}) a significant reduction of ATP binding affinity (Figure 2B) is produced by TG (K_d = 74 μM) or CPA (K_d = 189 μM) at inhibitory concentrations. An even greater reduction of ATP binding affinity by TG was previously derived from competitive experiments with an azido derivative of TNP-ATP (*24*). In fact, it is known that the enzyme headpiece is stabilized by TG in a closed configuration (i.e., E2−TG), as demonstrated by Toyoshima and Nomura (*9*).

ATP Utilization for Formation of Phosphorylated Enzyme Intermediate. To obtain a term of comparison for the binding experiments described above, we performed measurements of ATP utilization for formation of phosporylated enzyme intermediate. Figure 3A shows that, in the presence of Ca^{2+}, maximal levels of phosphorylation are obtained within 5 s incubation at 2−3 °C temperature. This is due to the much higher rates of phosphoenzyme formation as compared with

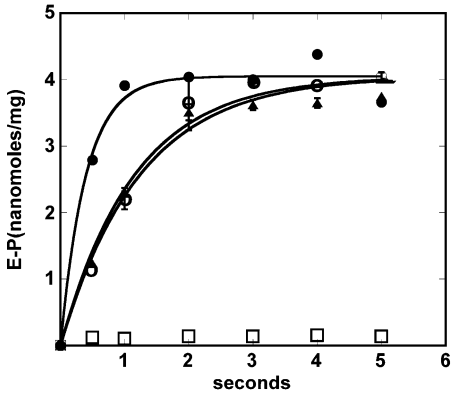

FIGURE 4: Ca^{2+} requirement for enzyme phosphorylation by ATP. The reaction was started by addition of 10 μM ATP to enzyme preincubated with Ca^{2+} (●), addition of 10 μM ATP and 1 mM Ca^{2+} to enzyme preincubated with 1 mM EGTA (○), addition of 1 mM Ca^{2+} to enzyme preincubated with 1 mM EGTA and 10 μM ATP (▲), and addition of 10 μM ATP to enzyme preincubated with 1 mM EGTA in the absence of Ca^{2+} (□). Reaction conducted as described in Materials and Methods, at 2 °C.

phosphoenzyme cleavage at low temperature. Maximal levels of phosphoenzyme, nearing the stoichiometry of available ATPase sites, are obtained with 10 μM ATP (Figure 3B).

No significant levels of ATP utilization are observed in the absence of Ca^{2+}. In fact, the rate-limiting enzyme activation by Ca^{2+} is demonstrated by a delay of phosphoenzyme formation when ATP and Ca^{2+} are added simultaneously to enzyme deprived of Ca^{2+}, as compared with addition of ATP to enzyme preincubated with Ca^{2+} (Figure 4). It is noteworthy that addition of Ca^{2+} to enzyme preincubated with ATP in the absence of Ca^{2+} yields the same delay, indicating that ATP binding in the absence of Ca^{2+} (under our conditions, at pH 7.0) does not bypass or facilitate the Ca^{2+}-dependent transition. Notably, at acid pH, ATP may facilitate the E2 to E1−2Ca^{2+} transition (*38*, *14*).

Nucleotide Binding and Conformational Effects in the Presence of Ca^{2+}. A most important point of interest is whether binding of nucleotide produces a substrate-induced fit, preliminary to the phosphoryl transfer reaction. However, ATP binding to E1·2Ca^{2+} cannot be measured directly because of its rapid consumption by the Ca^{2+}-activated enzyme. Furthermore, simple binding measurements do not distinguish the productive substrate complex at the catalytic site from nucleotide bound in alternative configurations. We therefore extended previous studies of specific conformational effects produced by the ATP analogue AMPPCP, as revealed by the pattern of ATPase protein digestion with proteinase K (*26*, *29*). In fact, accessible proteinase K digestion sites are located within the loops connecting the A domain to the membrane regions and become protected as the enzyme undergoes specific conformational changes (*29*, *31*), and the A domain rotates and/or bends (Figure 1). Even though its structure is analogous to that of ATP, AMPPCP is not utilized for covalent transfer of its terminal phosphate, so that the conformational effects of its binding to the ATPase can be studied under equilibrium conditions.

Figure 5 shows that electrophoresis of ATPase protein subjected to limited digestion with proteinase K (*30*) in the absence of Ca^{2+} exhibits 95 and 83 kDa bands, corresponding to fragments intervening between Lys120 (in the link between the A domain and M2) and the carboxyl terminus,

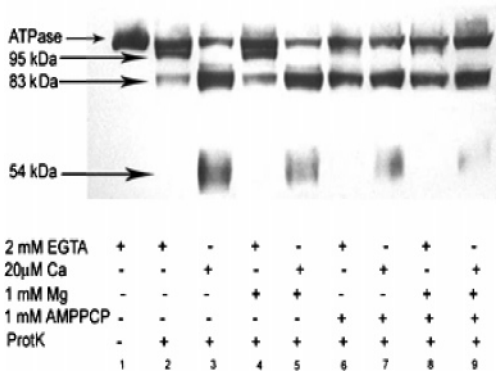

FIGURE 5: Partial digestion of ATPase with proteinase K. Effects of Ca^{2+}, Mg^{2+}, and AMPPCP. Digestion with Proteinase K and electrophoresis as explained in Materials and Methods, using 0.04 mg of ProtK/mL, for 10 min. The experiment shows that the ATPase band is optimally protected by AMPPCP when both Ca^{2+} and Mg^{2+} are present (compare lane 5 with lane 9).

and Glu243 (in the link between the A domain and M3) and the carboxyl terminus (Figure 1). In the presence of 20 μM Ca^{2+}, the digestion proceeds more rapidly, yielding a prominent 83 kDa band, and a 54 kDa band that corresponds to the segment between the Glu243 and Val734/Val747 proteolytic sites. In the absence of Ca^{2+}, AMPPCP does not protect digestion of the ATPase band but increases digestion of the 95 kDa, yielding an electrophoretic pattern with a more prominent 85 kDa band and no visible 54 kDa band. In the presence of 20 μM Ca^{2+}, AMP-PCP produces only modest protection (see below for high Ca^{2+}). In contrast, in the presence of 1 mM Mg^{2+} (no Ca^{2+} present) AMPPCP produces evident protection, which is even more evident if both Ca^{2+} (20 μM) and Mg^{2+} (1 mM) are present (Figure 5). In the absence of AMPPCP, Mg^{2+} show only slight protection of the 83 kDa band, in the absence or in the presence of Ca^{2+}. These diverse proteolytic patterns are due to changes in the accessibility and flexibility of peptide loops, which are related to displacement of the A domain and catalytically relevant conformational transitions (Figure 1).

We observed previously a similar protection in the presence of fluoroaluminate, which is optimized by the addition of ADP and Ca^{2+} (*27*) due to formation of an ADP−E1−AlF_x−$2Ca^{2+}$ complex. This protection is attributed to rotation and tilting of the "A" headpiece domain, whereby the proteolytic digestion sites (residing in the loops connecting the "A" domain to the transmembrane helices) are hidden from the medium or become rigid. The similar protection pattern produced by AMPPCP indicates that in the presence of Ca^{2+} and Mg^{2+} the enzyme−nucleotide complex acquires a conformation nearly identical to that of the fluoroaluminate phosphoenzyme analogue.

A distinct feature of the AMPPCP effect is the requirement for high (mM) nucleotide concentrations (Figure 6), as compared with the micromolar concentrations required for ATPase activation. Such a high ligand concentration requirement suggests that, under conditions of catalytic activation, nucleotide binding yields an unstable transition complex, preceding the covalent phosphoryl transfer (which does not occur when AMP-PCP is used instead of ATP). Dissociation of the complex is evidently prevented by second-order stabilization with high ligand concentrations. It is interesting

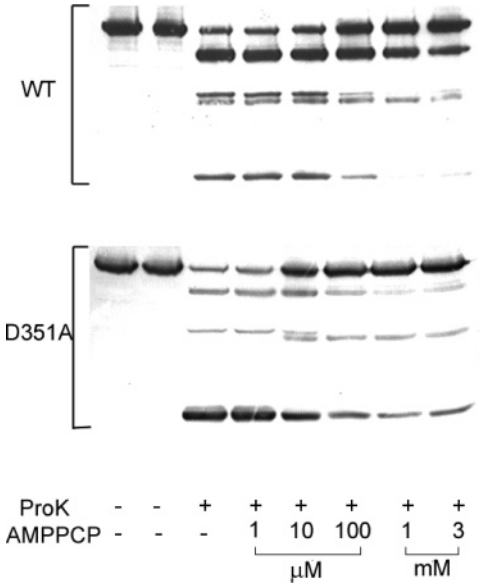

FIGURE 6: Partial digestion of ATPase with proteinase K. Protection by AMPPCP and concentration dependence. Digestion with Proteinase K and electrophoresis as explained in Materials and Methods, using 0.015 mg of ProtK/mL, for 40 min. There are 20 μM Ca^{2+} and 1 mM Mg^{2+} present in all samples. The experiment shows that protection by AMPPCP requires higher concentration when WT ATPase is used, as compared with the Asp351Ala mutant.

that the AMPPCP concentration required for the protective effect is much lower when the Asp351 is mutated to Ala (Figure 6).

Mg^{2+} enhances AMPPCP protection in the presence of micromolar Ca^{2+} concentrations, but does not appear to be a major requirement when high concentrations (mM) of Ca^{2+} are present (not shown), most likely due to Ca^{2+} substitution for Mg^{2+}. However, in the absence of AMPPCP, 10 mM Ca^{2+} affords little or no protection. It should be understood that the Mg^{2+} requirement is not limited to a structural role, but includes metal ion assistance in the general acid−base catalytic mechanism of the phosphorylation reaction with ATP, as well as with P_i in the reverse direction of the cycle.

ADP Binding. We then proceeded to determine to what extent ADP is a good leaving product following phosphoryl transfer from ATP to the enzyme. To this aim, we preequilibrated the enzyme with KF, $AlCl_3$, and Ca^{2+} to obtain the fluoroaluminate phosphoenzyme analogue with Ca^{2+} bound (E1−AlF_x−$2Ca^{2+}$). Fluoroaluminate reacts stoichiometrically with all the ATPase molecules in the incubation mixture and produces complete catalytic inactivation, as demonstrated by biochemical (*39*, *27*) and crystallographic experiments (*11*, *12*). Figure 7 shows that ADP has a high binding affinity ($K_d = 4$ μM) for E1−AlF_x−$2Ca^{2+}$ (transition state analogue of E1−P−$2Ca^{2+}$). In contrast, the affinity for ADP binding to the fluoroaluminate phosphoenzyme analogue is low if Ca^{2+} is omitted to obtain E2−AlF_x (transition state analogue of E2−P). Fitting of the experimental points obtained with E2−AlF_x, E2, or E1−$2Ca^{2+}$, based on the known maximal number of binding sites, yields very low affinity constants. These measurements demonstrate clearly that the ADP product has high affinity for the transition state analogue of E1−P−$2Ca^{2+}$, but it becomes a good leaving product as the phosphoenzyme undergoes the E1−P to E2−P transition.

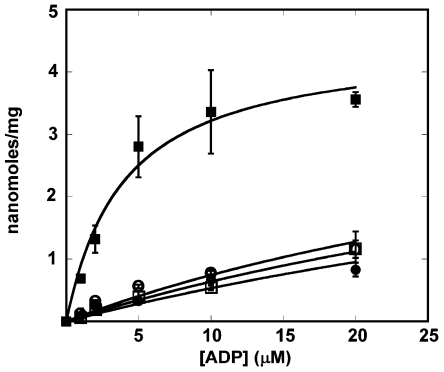

FIGURE 7: ADP binding to the ATPase and to the fluoroaluminate analogue of the phosphorylated enzyme intermediate, in the absence and in the presence of Ca^{2+}. (^{14}C)-ADP was mixed into the reaction mixture and incubated for 30 min at 20 °C and then filtered. Control with no fluroaluminate or Ca^{2+} (○); control with no fluoroaluminate, but with 20 μM Ca^{2+} (●); fluoroaluminate with no Ca^{2+} (□); fluoroaluminate with 20 μM Ca^{2+} (■).

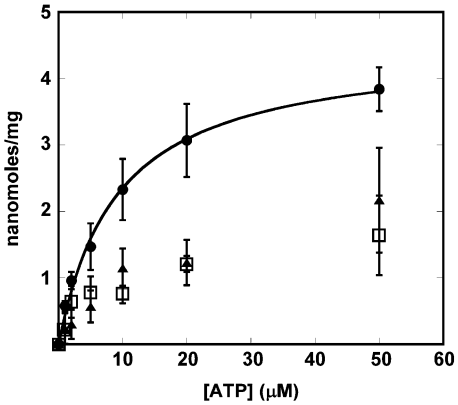

FIGURE 8: ATP binding to the fluoroaluminate analogue of the phosphorylated enzyme intermediate. SR vesicles were incubated for 30 min with 2 mM KF and 100 μM $AlCl_3$ at 2 °C, as described in Materials and Methods. ATP was added rapidly to the medium at 2 °C, and the mixture was filtered after 10 s incubation. Control with no fluroaluminate or Ca^{2+} (●); fluoroaluminate with no Ca^{2+} (▲); fluoroaluminate with 20 μM Ca^{2+} (□).

ATP Binding to the Fluoroaluminate Analogue of EP. To clarify the known enhancement of steady-state ATPase activity by high ATP concentrations (above the K_m range), we studied ATP binding to the phosphoenzyme intermediate analogue obtained with fluoroaluminate in the presence ($E1-AlF_x-2Ca^{2+}$) or in the absence of Ca^{2+} ($E2-AlF_x$). The binding affinity observed under these conditions (Figure 8) was considerably lower (*37*), and determination of binding at high ATP concentrations was prevented by the unfavorable noise-to-signal ratio. Nevertheless, it is clear that ATP can still bind to the phosphoenzyme intermediate analogue, although with low affinity. To test the functional consequence of low-affinity ATP binding to the phosphoenzyme, we then measured the decay rate of phosphoenzyme obtained by a 5 s incubation of Ca^{2+}-activated ATPase with 10 μM radioactive γ-^{32}P-ATP at 2 °C (i.e., $E1-P-2Ca^{2+}$). Under these conditions, a steady level of ^{32}P-phosphoenzyme corresponding to nearly all the ATPase molecules in the reaction medium is obtained. Following this 5 s incubation, we initiated radioactive phosphoenzyme decay by a chase with 10 mM EGTA to prevent further activation of enzyme by Ca^{2+}, or with 10 mM EGTA and 1 mM nonradioactive ATP. Figure 9 shows that the decay is faster when the chase

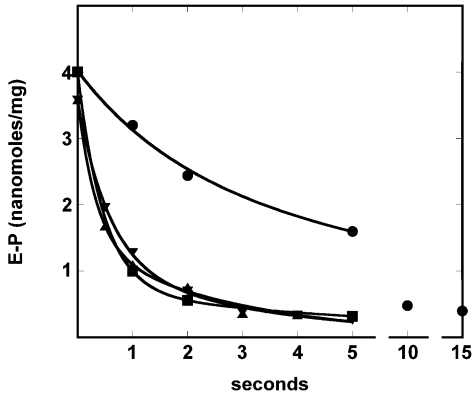

FIGURE 9: Decay of radioactive phospoenzyme obtained with ATP or P_i. Decay of phosphoenzyme made with ATP was initiated by a chase with 10 mM EGTA (●) or 1 mM nonradioactive ATP and 10 mM EGTA(■). Decay of phosphoenzyme made with P_i was initiated by a chase with 50 mM P_i (▲) or 50 mM P_i and 1 mM ATP (▼). In both cases, the temperature of the chase was 2 °C. The time curve following the EGTA chase (●) includes additional points up to 15 s, which were used for exponential fitting, and are not included in the graphics curve to avoid excessive compression of the time scale for the other curves.

includes millimolar concentrations of ATP, as compared with EGTA alone. In fact, the experimental points are best fitted by two exponentials. The decay in the presence of EGTA has an initial fast component (2 s^{-1}) that accounts for only 15% of the curve, and a slower component (0.16 s^{-1}) that accounts for 85%. In contrast, in the presence of 1 mM ATP, the fast component (2.0 s^{-1}) accounts for 84%, and the slow component (0.13 s^{-1}) accounts for 16% of the decay.

In a parallel set of experiments, we studied the decay of phosphoenzyme obtained with ^{32}P-P_i in the absence of Ca^{2+} (i.e., E2−P). In this case, the decay of radioactive phosphoenzyme was initiated by the addition of excess nonradioactive P_i or excess nonradioactive P_i and 1 mM ATP. Figure 9 shows that, in both cases, the decay of E2−P occurs faster than the decay of the $E1-P-2Ca^{2+}$ with no added ATP, indicating that in the later case decay is delayed by the E1−P to E2−P transition. Furthermore, decay of phosphoenzyme obtained with ^{32}P-P_i in the absence of Ca^{2+} occurs with nearly identical kinetics as the $E1-P-2Ca^{2+}$ decay in the presence of mM ATP. Considering the low-affinity ATP binding to the E-P analogue demonstrated in Figure 8, the experiment shown in Figure 9 indicates that low-affinity binding of ATP to $E1-P-2Ca^{2+}$ accelerates the E1−P to E2−P transition and thereby the consequent phosphoenzyme decay. This is consistent with earlier reports on the effect of ATP secondary binding on phosphoenzyme decay (*40*−*42*).

Conformational Effect of Thapsigargin. We extended the experiments with proteinase K to check whether TG may influence the pattern of ATPase digestion. Previous experiments on digestion of native sarcoplasmic reticulum ATPase with proteinase K, followed by electrophoresis and staining with Coomassie Blue, indicated that TG hardly affected the resistance of ATPase to proteolytic attack (*31*). In our experiments, we used recombinant SERCA1, followed by detection of electrophoretic fragments by Western blots, using an antibody that reacts with the carboxy terminus of the enzyme protein. As immunostaining yields a stoichiometric rather than protein mass quantitation, we were able to follow the digestion pattern down to small fragments. We found (Figure 10) that (in the absence of Ca^{2+}) the ATPase

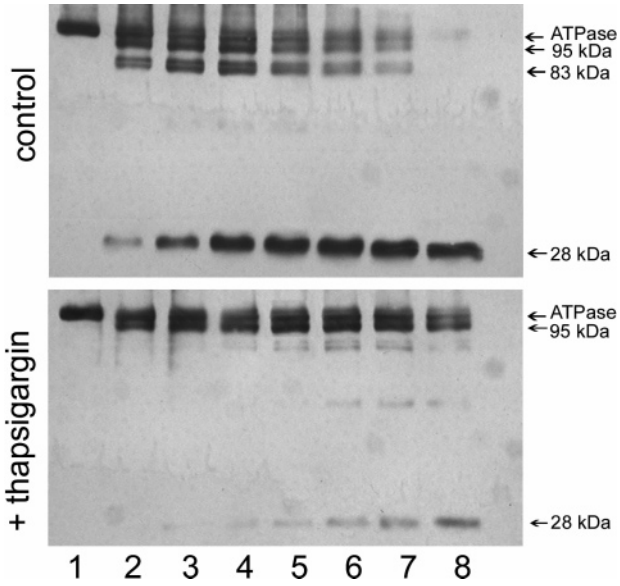

FIGURE 10: Partial digestion of ATPase with proteinase K. Effect of TG. Digestion with Proteinase K and electrophoresis as explained in Materials and Methods, using 0.04 mg of ProtK/mL. The reaction mixture contained 1.0 mM EGTA, 10 μM Ca^{2+} (endogenous), and 1.0 μM TG when indicated. The time of incubation with Proteinase K was for 0 (lane 1), 10 (lane 2), 20 (lane 3), 30 (lane 4), 40 (lane 5), 50 (lane 6), 60 (lane 7), and 90 (lane 8) min.

protein, the 95 kDA fragment (cut around K120 in the A domain−M2 link (*30*)), and the 83 kDa fragments were moderately protected by TG. However, the large yield of a small 28 kDa fragment (cut around V747 or V734 in the M5 helix (*30*)) produced in the control samples was not observed when TG was present in the reaction mixture. It is then apparent that the ATPase conformation is significantly constrained by TG binding. Therefore, proteolytic sites are protected.

DISCUSSION

It is now useful to consider the questions posed in the introduction to this article, providing explanations based on the experimental findings as follows:

1. Does ATP Bind to the Enzyme with High Affinity in the Absence of Ca^{2+}, and Why Is It Utilized only in the Presence of Ca^{2+}? A high affinity (K_d = 5−9 μM) for ATP binding is obtained by direct measurements in the absence of Ca^{2+} (Figure 1A, and refs *35*−*37*). An even higher affinity was derived from competition studies with an azido derivative of TNP-ATP (*24*). This range of binding affinity in the absence of Ca^{2+} is consistent with the ATP concentration dependence of phosphoenzyme formation in the presence of Ca^{2+}, when related kinetic constants are taken into account. However, ATP is not utilized for phosphoenzyme formation in the absence of Ca^{2+}, even if Mg^{2+} is present (*43*). This indicates that the bound ATP acquires a position permitting covalent transfer of its terminal phosphate only in the presence of Ca^{2+}. The occurrence of ATP (Figure 8) binding to the fluoroaluminate phosphoenzyme analogue (where the phosphorylation site is already occupied) demonstrates that an extended phosphate chain configuration, reaching Asp351 for catalytic interaction, is not a requirement for ATP binding. In fact, even in the presence of Ca^{2+}, bound ATP can acquire a configuration with a folded phosphate chain

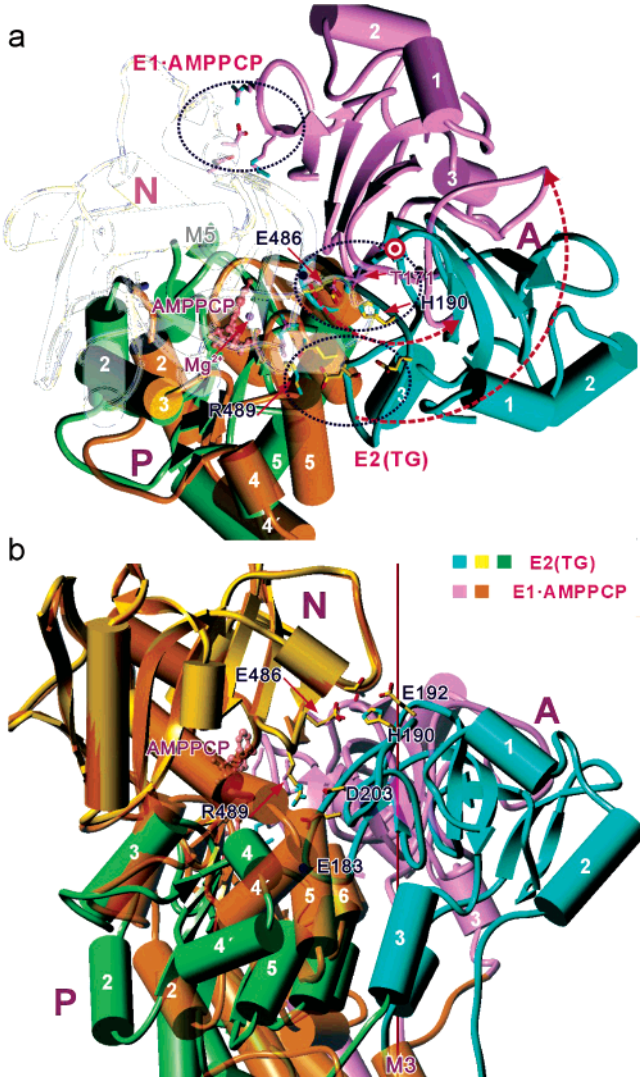

FIGURE 11: Arrangement of the cytoplasmic domain in the E2−AMPPCP(TG) (2DQS) and E1−AMPPCP−2Ca^{2+} (1VFP) crystal structures. The structures are superimposed by fitting the N domain, which shows little conformational changes between the two structures. The A domain movement between the two states is largely approximated by a 110° rotation (indicated by dotted arrows in panel a around an axis (a, thin red rod; b, double circles) nearly perpendicular to the membrane. Views are along the rotation axis (a) and normal to it (b). The residues forming hydrogen bonds between A and N domains are clustered (dotted circles) and shown in stick representation. Only E486 is involved in either structure.

reaching Thr441 rather than Asp351 (*44*). Therefore, while interaction of the adenosine moiety with the N domain is a basic feature of nucleotide binding to the ATPase, the ATP γ-phosphate is only permitted to reach Asp351 through a Ca^{2+}-dependent and specific substrate-induced conformation (Figure 1). Acquisition of this ATPase conformation entails a large inclination of the N domain toward the P domain (Figure 11), and bending of the P domain with stabilization by Mg^{2+}. Binding of Mg^{2+} in the P domain is likely to be cooperative, since it requires γ-phosphate as one of the coordinating oxygen atoms (*11*, *12*). The large inclination of the N domain (which can only be permitted by the opening of the A domain in the Ca^{2+}-induced conformation) allows cross-linking of the N and P domains by Arg560 via the ATP β-phosphate. Furthermore, bending of the P domain affects further the A domain, tilting it by ∼30° and placing

strain on the A domain−M3 helix loop. Thereby, a subsequent 110° rotation of the A domain is facilitated, in concomitance with the E1−P to E2−P transition.

Figure 11 shows that the space around the ATP phosphate chain is substantially narrower in the AMPPCP−E1−2Ca^{2+} than in the recently obtained (PDB 2DQS; see also ref *14*) AMPPCP−E2(TG) crystal structure. That is because, in the AMPPCP−E2(TG) structure, a suitable bending of the P domain (to allow adjustment of the bound ATP) is sterically hindered by the A domain. As shown in Figure 11b, the loop containing the TGES signature sequence interferes with the P5−P6 helices. Furthermore, as the A domain is wedged into the space between the N and P domains, further bending of the N domain appears unlikely (Figure 11b).

In the AMPPCP−E2(TG) structure, the nucleotide binds to the same place as in the AMPPCP−E1−2Ca^{2+} complex, but the phosphate chain is in a folded configuration, rather distant from Asp351 in the P domain (Figure 1). The two structures are similar, with the exception of a TGES loop movement that interferes with the proper interaction of the A domain with the P domain in the AMPPCP−E2(TG) complex. Therefore, interference with a productive phosphate configuration is most likely due to lack of stabilization by P domain residues and Mg^{2+}. It is clear that the Ca^{2+}-induced headpiece opening is necessary to eliminate the interference of the TGES loop with the movement of the P domain. It is conceivable that opening of the headpiece domain may occur faster when Ca^{2+} binds in the presence of bound ATP, at least under some conditions.

Comparing the AMPPCP−E2(TG) to the AMPPCP−E1−2Ca^{2+} crystal structure, displacement of the A domain can be represented by a 110° rotation around an axis approximately perpendicular to the membrane (double circle in Figure 11a and red dot in Figure 11b) with a ∼5 Å translation. As a result, the interface between the A domain and the N domain is totally different in the two structures, with Glu486 as the only residue contributing in both states (Figure 11a).

Considering that (a) direct measurements (Figure 2) indicate that ATP binds with high affinity in the absence of Ca^{2+}; (b) Ca^{2+} is nevertheless required for ATP utilization (Figure 4); and (c) the AMPPCP−E1−2Ca^{2+} structure presents significant changes relative to both E1−2Ca^{2+} and AMPPCP−E2(TG) (Figure 1; refs *10*, *11*, *14*), we conclude that the phosphate chain of bound ATP acquires the extended and productive configuration (including Mg^{2+} engagement: Figure 1) as a consequence of two consecutive and interdependent conformational changes produced by Ca^{2+} and ATP binding to the enzyme.

2. Why Does Stabilization of AMPPCP−E1−2Ca^{2+} Require High Ligand Concentration? The *crystal structures* of AMPPCP−E1−2Ca^{2+} (analogue of the substrate−enzyme complex) and ADP−E1−AlF_4−2Ca^{2+} (analogue of the phosphoryl transfer transition state) are nearly identical (Figure 12), showing that substrate binding has already produced a productive configuration at the catalytic site (i.e., suitable for the phosphoryl transfer reaction), as well as occlusion of the 2 Ca^{2+} bound in the transmembrane region (*10*, *12*). This is a very important substrate-induced conformational change, triggered by AMPPCP binding to E1−2Ca^{2+}. Yet, in *solution experiments*, it is very difficult to demonstrate Ca^{2+} occlusion in the presence of AMPPCP,

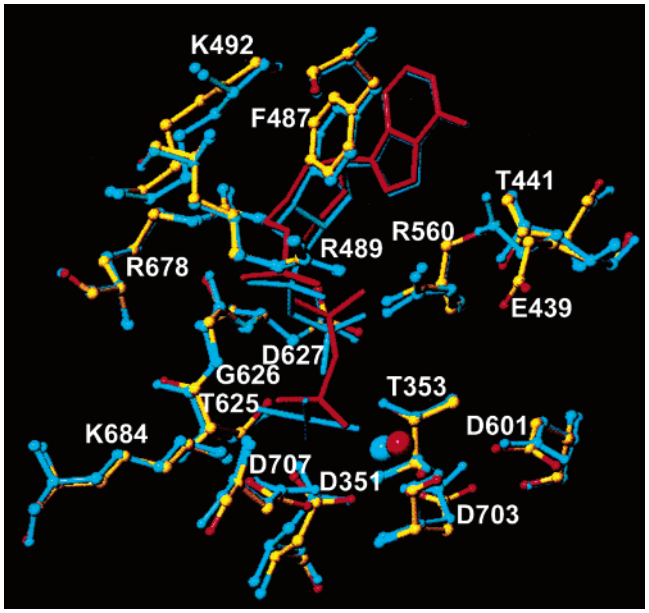

FIGURE 12: Alignment of key residues and substrate in AMPPCP−E1−2Ca^{2+} (1VFP) and ADP−E1−AlF_x−2Ca^{2+} (1WPE). Amino acid residues are shown in atom color, AMPPCP and Mg^{2+} in red for AMPPCP−E1−2Ca^{2+}; amino acid residues, ADP, aluminum fluoride, and Mg^{2+} are shown in blue for ADP−E1−AlF_x−2Ca^{2+}. Not withstanding a nearly identical conformation, AMPPCP−E1−2Ca^{2+} is unstable in solution, while ADP−E1−AlF_x−2Ca^{2+} is stable (see text).

while it is quite easy to show Ca^{2+} occlusion in the presence of fluoroaluminate and ADP (*27*, *28*). Furthermore, proteinase K protection experiments indicate that stabilization of the AMPPCP-induced conformation requires high (mM) concentrations of nucleotide, well above the micromolar requirement for ATP binding to the enzyme in the absence of Ca^{2+} (Figure 2), and above the micromolar ATP requirement for enzyme phosphorylation in the presence of Ca^{2+} (Figure 3). In addition, stabilization by high Ca^{2+} is also observed, which may be related to replacement of Mg^{2+} bound to the P domain by Ca^{2+} (*45*), as its larger radius is presumably required to cope with a longer distance between the metal and the oxygen atom of the γ-phosphate, as compared with the fluorine atom of AlF_x.

Overall, our experiments indicate that the nucleotide-dependent, productive enzyme conformation is unstable in solution. Electrostatic repulsion between γ phosphate and Asp351 (Figure 6) and additional neighboring residues (*46*) contributes to the instability of the productive phosphate configuration. Considering the nearly identical conformations (Figure 12) of AMPPCP−E1−2Ca^{2+} (analogue of the substrate−enzyme complex) and ADP−E1−AlF_4−2Ca^{2+} (analogue of the phosphoryl transfer transition state), a very interesting difference is the *instability* of the former *in solution*, as compared to the *stability* of the latter. To explain this difference, we consider that when we use AMPPCP (inactive substrate analogue) in *solution* experiments, the binding complex is observed under *equilibrium* conditions. As the ATPase binding constant for the nucleotide substrate is of the order of 10^6 M^{-1}, it is apparent that the 10^{-3} M AMPPCP requirement is related to stabilization provided by binding energy (RT ln 10^{-6} M^{-1} × 10^{-3} M = 4.2 Kcal mol^{-1}). On the other hand, when ATP is used, the unstable productive conformation is transient and proceeds to covalent

phosphoryl transfer to the enzyme. In this case, we deal with *steady-state turnover* (rather than *equilibrium*), and an analogous requirement (4 Kcal mol^{-1}) is observed as energy of activation, which can be estimated from the temperature dependence of the phosphorylation reaction rates (*47* and Figure 3A). Considering that the equilibrium constant for the phosphorylation reaction is nearly 1, it is evident that significant activation energy is required to attain the productive enzyme−substrate complex conformation, but the phosphoryl transfer reaction then yields a stable product.

3. Is ADP a Strong or Weak Ligand, and Is It a Good Leaving Group Following Phosphoryl Transfer from ATP to the Enzyme? Does Low-Affinity ATP Binding Influence the Kinetics of the ATPase Cycle? We found that ADP binds (Figure 7) with rather high affinity to the fluoroaluminate analogue of the phosphoenzyme in the presence of Ca^{2+} (i.e., $E1-AlF_x-2Ca^{2+}$), This indicates that, following covalent phosphoryl transfer, the electrostatic repulsion between ATP γ-phosphate and Asp351 is relieved, thereby conferring stability to the ADP product. In contrast, the affinity of ADP for the fluoroaluminate analogue becomes significantly lower in the absence of Ca^{2+} (i.e., $E2-AlF_x$). This is in very good agreement with crystal structures showing that the "A" domain rotates upon the E1−P to E2−P transition, filling the space previously occupied by ADP (*11*). Therefore, dissociation of the ADP product occurs as the phosphorylated enzyme intermediate undergoes the subsequent conformational transition (Figure 1).

An important finding, in this regard, is the occurrence of low-affinity ATP binding to the fluoroaluminate analogue of the phosphorylated intermediate (i.e., $E1-AlF_x-2Ca^{2+}$ or $E2-AlF_x$). This is in agreement with the observed competitive inhibition by ATP on ezyme phosphorylation with P_i (*48*). Our experiments suggest that ATP, at 0.1−1.0 mM concentrations, binds again to the phosphorylated intermediate in exchange for ADP. In this case, low-affinity ATP binding to $E1-P-2Ca^{2+}$ relies on interaction with the adenosine binding pocket, without intrusion of the phosphate chain into the phosphorylation site. The presence of ATP on the N domain has evidently a destabilizing effect on E1-P, with consequent acceleration of the E1−P to E2−P transition (Figure 9). This explains the second rise of steady-state ATPase velocity produced by ATP above the K_m concentration range (*13*−*16*). It is noteworthy that such a kinetic effect of low-affinity ATP binding appears to be quite specific for the E1−P to E2−P transition. In fact, hydrolytic cleavage of E2−P is not affected (Figure 9).

4. Is the ATPase Headpiece Conformation Affected by TG Binding? When the AMPPCP−E2−TG and AMPPCP−$E1-2Ca^{2+}$ crystal structures are compared, it is apparent that productive (i.e., extended phosphate chain) binding of ATP (AMPPCP) and Mg^{2+} requires opening of the cytoplasmic headpiece, which is certainly realized following cooperative Ca^{2+} binding to the two high-affinity transmembrane sites. An important question is then related to the stability of the A and N domains interaction in the absence of Ca^{2+} (with no TG). In the E2−TG crystal structure, the A and N domains interaction is stabilized by several hydrogen bonds, including the His190 (A)−Glu486 (N), and Asp202 (A)−Arg489 (N) salt bridges (Figure 11). They are preserved in the recently obtained structure of E2(TG) with bound AMPPCP. On the other hand, we do not know how stable this interaction is in the absence of Ca^{2+} and TG. Considering that we observe rapid denaturation of the ATPase in the absence of Ca^{2+} (not shown), we anticipate that this association may not be very stable, particularly at high pH. Furthermore, TG has a clear protective effect against ATPase digestion with proteinase K (Figure 9). In particular, nearly complete protection of the digestion site on the M5 helix suggests that M5 moves substantially in the absence of TG; this movement will bring the P and N domains apart from the A domain, thereby opening the gathered headpiece. Thus, we expect that, in solution, the headpiece is open for a significant fraction of time even in the absence of Ca^{2+} when TG is absent. This explains why the affinity for ATP is lower when TG is present (Figure 2).

In conclusion, our experiments indicate that nucleotide binding occurs through initial interaction of the adenosine moiety with the N domain of the ATPase, even in the absence of Ca^{2+} or Mg^{2+}. However, a productive substrate−enzyme complex is produced through two sequential and interdependent conformational effects produced by Ca^{2+} and ATP. Local electrostatic repulsion may be only overcome by protein conformational constraint, whereby the ATP γ-phosphate is permitted to reach Asp351 to form a complex with Mg^{2+}. This yields an unstable conformation of the productive complex. Stabilization is subsequently obtained through the covalent phosphoryl transfer reaction. This is consistent with extensive theoretical studies indicating that, generally, the most important catalytic factor is electrostatic *preorganization* of the enzyme active site (*49*). Following covalent phosphoryl transfer, the ADP product is released, and secondary ATP binding to the phosphoenzyme may occur with lower affinity, thereby accelerating further conformational transitions and turnover of the phosphoenzyme.

REFERENCES

1. MacLennan, D. H., Brandl, C. J., Korczak, B., and Green, N. M. (1985) Amino-acid sequence of a $Ca^{2+} + Mg^{2+}$-dependent ATPase from rabbit muscle sarcoplasmic reticulum, deduced from its complementary DNA sequence, *Nature 316*, 696−700.
2. Zhang, P., Toyoshima, C., Yonekura, K., Green, N. M., and Stokes, D. L. (1998) Structure of the calcium pump from sarcoplasmic reticulum at 8-Å resolution. *Nature 392*, 835−839.
3. de Meis, L., and Vianna, A. L. (1979) Energy interconversion by the Ca^{2+}-dependent ATPase of the sarcoplasmic reticulum. *Annu. Rev. Biochem. 48*, 275−292.
4. Moller, J. V., Juul, B., and le Maire, M. (1996) Structural organization, ion transport, and energy transduction of P-type ATPases, *Biochim. Biophys. Acta 1286*, 1−51.
5. Andersen, J. P., and Vilsen, B. (1998) Structure-function relationships of the calcium binding sites of the sarcoplasmic reticulum Ca(2+)-ATPase, *Acta Physiol. Scand., Suppl. 643*, 45−54.
6. Inesi, G., Lewis, D., Nikic, D., and Kirtley, M. E. (1992) Long-range intramolecular linked functions in the calcium transport ATPase, *Adv. Enzymol. 157*, 185−215.
7. Bigelow, D. J., and Inesi, G. (1992) Contributions of chemical derivatization and spectroscopic studies to the characterization of the Ca^{2+} transport ATPase of sarcoplasmic reticulum, *Biochim. Biophys. Acta 1113*, 323−338.
8. Toyoshima, C., Nakasako, M., Nomura, H., and Ogawa, H. (2000) Crystal structure of the calcium pump of sarcoplasmic reticulum at 2.6 Å resolution, *Nature 405*, 647−655.
9. Toyoshima, C., and Nomura, H. (2002) Structural changes in the calcium pump accompanying the dissociation of calcium, *Nature 418*, 605−611.
10. Toyoshima, C., and Mizutani, T. (2004) Crystal structure of the calcium pump with a bound ATP analogue. *Nature 430*, 529−535.

11. Toyoshima, C., Nomura, H., and Tsuda, T. (2004) Lumenal gating mechanism revealed in calcium pump crystal structures with phosphate analogues, *Nature 432*, 361−368.
12. Sorensen, T. L.-M., Moller, J. V., and Nissen, P. (2004) Phosphoryl transfer and calcium ion occlusion in the calcium pump. *Science 304*, 1672−1675.
13. Olesen, C., Sorensen, T. L., Nielsen, R. C., Moller, J. V., and Nissen, P. (2004) Dephosphorylation of the calcium pump coupled to counterion occlusion. *Science 306*, 2251−2255.
14. Jensen, A. L., Sorensen, T. L., Olesen, C., Moller, J. V., and Nissen, P. (2006) Modulatory and catalytic modes of ATP binding by the calcium pump. *EMBO J. 25*, 2305−2314.
15. Inesi, G., Goodman, J. J., and Watanabe, S. (1967) Effect of diethyl ether on the adenosine triphosphatase activity and the calcium uptake of fragmented sarcoplasmic reticulum of rabbit skeletal muscle. *J. Biol. Chem. 242*, 4637−4644.
16. Yamamoto, T., and Tonomura, Y. (1967) Reaction mechanism of the Ca^{2+} dependent ATPase of sarcoplasmic reticulum from skeletal muscle. I. Kinetic studies. *J. Biochem. (Tokyo) 62*, 558−575.
17. Verjovski-Almeida, S., and Inesi, G. (1979) Fast-kinetic evidence for an activating effect of ATP on the Ca^{2+} transport of sarcoplasmic reticulum ATPase. *J. Biol. Chem. 254*, 18−21.
18. Lund, S., and Moller, J. V. (1988) Biphasic kinetics of sarcoplasmic reticulum Ca^{2+}-ATPase and the detergent-solubilized monomer. *J. Biol. Chem. 263*, 1654−1664.
19. Bastide, F., Meissner, G., Fleischer, S., and Post, R. L. (1973) Similarity of the active site of phosphorylation of the adenosine triphosphatase from transport of sodium and potassium ions in kidney to that for transport of calcium ions in the sarcoplasmic reticulum of muscle. *J. Biol. Chem. 248*, 8385−8391.
20. Degani, C., and Boyer, P. D. (1973) A borohydride reduction method for characterization of the acyl phosphate linkage in proteins and its application to sarcoplasmic reticulum adenosine triphosphatase. *J. Biol. Chem. 248*, 8222−8226.
21. Mitchinson, C., Wilderspin, A. F., Trinnaman, B. J., and Green, N. M. (1982) Identification of a labelled peptide after stoicheiometric reaction of fluorescein isothiocyanate with the Ca^{2+}-dependent adenosine triphosphatase of sarcoplasmic reticulum. *FEBS Lett. 146*, 87−92.
22. Maruyama, K., Clarke, D. M., Fujii, J., Inesi, G., Loo, T. W., and MacLennan, D. H. (1989) Functional consequences of alterations to amino acids located in the catalytic center (isoleucine 348 to threonine 357) and nucleotide-binding domain of the CA^{2+}-ATPase of sarcoplamic reticulum, *J. Biol. Chem. 264*, 13038−13042.
23. Clarke, D. M., Loo, T. W., and MacLennan, D. H. (1990) Functional consequences of alterations to amino acids located in the nucleotide-binding domain of the Ca^{2+}-ATPase of sarcoplasmic reticulum. *J. Biol. Chem. 265*, 22223−22227.
24. McIntosh, D. B., Woolley, D. G., Vilsen, B., and Andersen, P. J. (1996) Mutagenesis of segment 487Phe-Ser-Arg-Asp-Arg-Lys492 of sarcoplasmic reticulum Ca^{2+}-ATPase produces pumps defective in ATP binding. *J. Biol. Chem. 271*, 25778−25789.
25. Clausen, J. D., McIntosh, D. B., Vilsen, B., Woolley, D. G., and Andersen, J. P. (2003) Importance of conserved N-domain residues Thr441, Glu442, Lys515, Arg560, and Leu562 of sarcoplasmic reticulum Ca^{2+}-ATPase for MgATP binding and subsequent catalytic steps. Plasticity of the nucleotide-binding site. *J. Biol. Chem. 278*, 20245−20258.
26. Ma, H., Inesi, G., and Toyoshima C. (2003) Substrate-induced conformational fit and headpiece closure in the Ca^{2+}ATPase (SERCA). *J. Biol. Chem. 278*, 28938−28943.
27. Inesi, G., Ma, H., Lewis, D., and Xu, C. (2004) Ca^{2+} occlusion and gating function of Glu309 in the ADP-fluoroaluminate analog of the Ca^{2+}-ATPase phosphoenzyme intermediate. *J. Biol. Chem. 279*, 31629−31637.
28. Picard, M., Toyoshima, C., and Champeil, P. (2005) The average conformation at micromolar [Ca^{2+}] of Ca^{2+}-ATPase with bound nucleotide differs from that adopted with the transition state analog ADP. AlFx or with AMPPCP under crystallization conditions at millimolar [Ca^{2+}]. *J. Biol. Chem. 280*, 18745−18754.
29. Danko, S., Yamasaki, K., Daiho, T., Suzuki, H., and Toyoshima, C. (2001) Organization of cytoplasmic domains of sarcoplasmic reticulum Ca(2+)-ATPase in E(1)P and E(1)ATP states: a limited proteolysis study. *FEBS Lett. 505*, 129−135.
30. Juul, B., Turc, H., Durand, M. L., Gomez de Gracia, A., Denoroy, L., Moller, J. V., Champeil, P., and le Maire, M. (1995) Do transmembrane segments in proteolyzed sarcoplasmic reticulum Ca(2+)-ATPase retain their functional Ca^{2+} binding properties after removal of cytoplasmic fragments by proteinase K? *J. Biol. Chem. 270*, 20123−20134.
31. Danko, S., Daiho, T., Yamasaki, K., Kamidochi, M., Suzuki, H., and Toyoshima, C. (2001) ADP-insensitive phosphoenzyme intermediate of sarcoplasmic reticulum Ca(2+)-ATPase has a compact conformation resistant to proteinase K, V8 protease and trypsin. *FEBS Lett. 489*, 277−282.
32. Eletr, S., and Inesi, G. (1972) Phospholipid orientation in sarcoplasmic membranes: spin-label ESR and proton MNR studies. *Biochim. Biophys. Acta 282*, 174−179.
33. Karin, N. J., Kaprielian, Z., and Fambrough, D. M. (1989) Expression of avian Ca^{2+}-ATPase in cultured mouse myogenic cells. *Mol. Cell. Biol. 9*, 1978−1986.
34. Zhang, Z., Lewis, D., Strock, C., Inesi, G., Nakasako, M., Nomura, H., and Toyoshima C. (2000) Detailed characterization of the cooperative mechanism of Ca^{2+} binding and catalytic activation in the Ca^{2+} transport (SERCA) ATPase. *Biochemistry 39*, 8758−8767.
35. Dupont, Y. (1977) Kinetics and regulation of sarcoplasmic reticulum ATPase. *Eur. J. Biochem. 72*, 185−190.
36. Meissner, G. (1973) ATP and Ca^{2+} binding by the Ca^{2+} pump protein of sarcoplasmic reticulum. *Biochim. Biophys. Acta 298*, 906−926.
37. Kubota, T., Daiho, T., and Kanazawa, T. (1993) Quasi-irreversible inactivation of the sarcoplasmic reticulum Ca(2+)-ATPase by simultaneous tight binding of magnesium and fluoride to the catalytic site *Biochim. Biophys. Acta 1163*, 131−143.
38. Mintz, E., Mata, A. M., Forge, V., Passafiume, M., and Guillain, F. (1995) The modulation of Ca^{2+} binding to sarcoplasmic reticulum ATPase by ATP analogues is pH-dependent. *J. Biol. Chem. 270*, 27160−27164.
39. Troullier, A., Girardet, J. L., and Dupont, Y. (1992) Fluoroaluminate complexes are bifunctional analogues of phosphate in sarcoplasmic reticulum Ca(2+)-ATPase. *J. Biol. Chem. 267*, 22821−22829.
40. McIntosh, D. B., and Boyer, P. D. (1983) Adenosine 5′-triphosphate modulation of catalytic intermediates of calcium ion activated adenosinetriphosphatase of sarcoplasmic reticulum subsequent to enzyme phosphorylation. *Biochemistry 22*, 2867−2875.
41. Bishop, J. E., Al-Shawi, M. K., and Inesi, G. (1987) Relationship of the regulatory nucleotide site to the catalytic site of the sarcoplasmic reticulum Ca^{2+}-ATPase. *J. Biol. Chem. 262*, 4658−4663.
42. Champeil, P., Riollet, S., Orlowski, S., Guillain, F., Seebregts, C. J., and McIntosh, D. B. (1988) ATP regulation of sarcoplasmic reticulum Ca^{2+}-ATPase. Metal-free ATP and 8-bromo-ATP bind with high affinity to the catalytic site of phosphorylated ATPase and accelerate dephosphorylation. *J. Biol. Chem. 263*, 12288−12294.
43. Lacapere, J. J., Bennett, N., Dupont, Y., and Guillain, F. (1990) pH and magnesium dependence of ATP binding to sarcoplasmic reticulum ATPase. Evidence that the catalytic ATP-binding site consists of two domains. *J. Biol. Chem. 265*, 348−353.
44. Hua, S., Inesi, G., Nomura, H., and Toyoshima, C. (2002) Fe^{2+}-catalyzed oxidation and cleavage of sarcoplasmic reticulum ATPase reveals Mg^{2+} and Mg^{2+}-ATP sites. *Biochemistry 41*, 11405−11410.
45. Shigekawa, M., Wakabyashi, S., and Nakamura, H. (1983) Effect of divalent cation bound to the ATPase of sarcoplasmic reticulum. Activation of phosphoenzyme hydrolysis by Mg^{2+}. *J. Biol. Chem. 258*, 14157−14161.
46. McIntosh, D. B., Clausen, J. D., Woolley, D. G., MacLennan, D. H., Vilsen, B., and Andersen J. P. (2004) Roles of conserved P domain residues and Mg^{2+} in ATP binding in the ground and Ca^{2+}-activated states of sarcoplasmic reticulum Ca^{2+}-ATPase. *J. Biol. Chem. 279*, 32515−32523.
47. Inesi, G., Kurzmack, M., and Lewis, D. (1988) Kinetic and equilibrium charcterization of an energy-transducing enzyme and its partial reactions. *Methods Enzymol. 157*, 154−190.
48. Masuda, A., and de Meis, L. (1973) Phosphorylation of the sarcoplasmic reticulum membrane by orthophosphate. Inhibition by calcium ions. *Biochemistry 12*, 4581−4585.
49. Olsson, M. H. M., Parson, W. W., and Warshel, A. (2006) Dynamical contributions to enzyme catalysis: critical tests of a popular hypothesis. *Chem. Rev. 106*, 1737−1756.

BI061255D